TITLE PAGE

Title: Interaction of Rabies Virus P-Protein with STAT Proteins is Critical to Lethal Rabies Disease.

Authors: L. Wiltzer[1, 2], K. Okada[3], S. Yamaoka[3], F. Larrous[4, 5], H. V. Kuusisto[2], M. Sugiyama[6], D. Blondel[7], H. Bourhy[4], D. A. Jans[2], N. Ito[6] and G. W. Moseley[1, 8]

Affiliations: [1]Viral Pathogenesis Laboratory and [2]Nuclear Signalling Laboratory, Department of Biochemistry and Molecular Biology, Monash University, Victoria 3800, Australia.

[3]The United Graduate School of Veterinary Sciences, Gifu University, Gifu, 501-1193, Japan.

[4]Institut Pasteur, Unit Lyssavirus Dynamics and Host Adaptation, Rue du docteur Roux, 75724 Paris, France.

[5]Université Paris Diderot, Sorbonne Paris Cité, Cellule Pasteur, 75013 Paris, France.

[6]Laboratory of Zoonotic Diseases, Faculty of Applied Biological Sciences, Gifu University, Gifu, 501-1193, Japan.

[7]Laboratoire de Virologie Moléculaire et Structurale, CNRS, UMR2472 Gif sur Yvette, France.

[8]Department of Biochemistry and Molecular Biology, Bio21 Institute, University of Melbourne, 30 Flemington Rd, Parkville, Victoria 3052, Australia.

Running title: P-STAT interaction is critical to rabies.

Word count: 3495 words

Funding: This work was supported by the National Health and Medical Research Council Australia [grant number 1003244 to G.W.M.]; Senior Principal Research Fellowship [grant 1002486 to D.A.J.]; Australian Research Council [grant number DP110101749 to G.W.M. and D.A.J.]; European Union Seventh Framework Programme [grant number 278433 to F.L. and H.B.]; Grants-in-Aid for Scientific Research from the Ministry of Education, Culture, Sports, Science and Technology, Japan [grant no. 23380179 and 24580424 to M.S. and N.I., respectively].

Acknowledgments: The authors would like to thank C. David and A. Brice for assistance with tissue culture, G. Le-Bury (CNRS) for help with Y2H assays, and A. Mansell (Monash Institute of Medical Research) for kindly providing the Flag-RIG-I plasmid. We would also like to thank Julia Young (Monash University) for discussions regarding the qRT-PCR data, and Johanna Fraser, Michelle Audsley, and Markus Bach (Monash University) for critical review of the manuscript. We also acknowledge the Monash Micro Imaging facility for provision of instrumentation, training and general support.

Conflict of interests: The authors report no conflict of interests.

Meetings: Partial information of this study was presented by the authors at the Annual Scientific Meeting of the Australasian Society for Immunology in December 2012 and the 15th International Negative Strand Virus Meeting in June 2013. However, due to the preparation of a provisional patent specification detailed information has been kept confidential.

Corresponding author: Gregory William Moseley; Viral Pathogenesis Laboratory, Department of Biochemistry and Molecular Biology, Bio21 Institute, University of

Melbourne, 30 Flemington Rd, Parkville, Victoria 3052, Australia; Email: gregory.moseley@unimelb.edu.au; Fax: +61 3 9348 1421; Phone: +61 3 8344 2288.

Alternate corresponding author: Naoto Ito; Laboratory of Zoonotic Diseases, Faculty of Applied Biological Sciences, Gifu University, 1-1 Yanagido, Gifu, 501-1193, Japan; Email: naotoito@gifu-u.ac.jp; Phone and Fax: +81 58 293 2949.

Abstract:

Background: Rabies virus (RABV) causes rabies disease resulting in >55,000 human deaths/year. The multifunctional RABV P-protein has essential roles in genome replication, and forms interactions with cellular STAT proteins that are thought to underlie viral antagonism of interferon-dependent immunity. However, the molecular details of P-protein-STAT interaction, and its importance to disease are unresolved.

Methods: Studies were performed using sequence/structure analysis, mutagenesis, immunoprecipitation, luciferase and qRT-PCR-based signaling assays, confocal microscopy and reverse genetics/in vivo infection.

Results: We identified a hydrophobic pocket of the P-protein C-terminal domain as critical to STAT-binding/antagonism. This interface was found to be functionally and spatially independent of the region responsible for N-protein interaction, which is critical to genome replication. Based on these findings, we generated the first mutant RABV lacking STAT-association. Growth of the virus in vitro was unimpaired, but it lacked STAT-antagonist function and was highly sensitive to interferon. Importantly, growth of the virus was strongly attenuated in brains of infected mice, producing no major neurological symptoms, compared with the invariably lethal wild-type virus.

Conclusions: These data represent direct evidence that P-protein-STAT interaction is critical to rabies, and provide novel insights into the mechanism by which RABV coordinates distinct functions in interferon antagonism and replication.

Key words:

Viral disease, interferon, signal transducers and activators of transcription, immune evasion, interferon antagonist, lyssavirus, rabies virus, Duvenhage virus, pathogenicity, replication

Introduction:

Rabies is an untreatable disease of humans, which has a case-fatality rate of almost 100% in non-vaccinated individuals [1]. The etiological agents of rabies are viruses of the globally distributed *Lyssavirus* genus, the best characterized of which is *rabies virus* (RABV) that infects diverse mammalian species with transmission to humans most commonly through bites from infected dogs. Seven other lyssaviruses, European bat lyssaviruses 1 and 2, Irkut virus, Australian bat lyssavirus (ABLV), Mokola virus (MOKV), and Duvenhage virus (DUVV), and most likely West Caucasian bat virus have caused lethal human rabies [2].

The principal host-cell response to viral infection is activation of the type-I interferon (IFNα/β)-mediated innate immune response. Following virus detection by receptors such as RIG-I, cells produce IFNα/β, which binds to type-I IFN receptors to activate cytoplasmic signal transducers and activators of transcription (STAT) 1 and 2 via phosphorylation at residues Y701 and Y690, respectively. Activated STAT1 and 2 heterodimerize and translocate to the nucleus where they activate IFN-stimulated genes (ISGs) including *ISG15* and *MxA*, which are important to the establishment of an antiviral state. The STATs are then dephosphorylated by nuclear phosphatases, and exported to the cytoplasm [3, 4].

Viruses counter these responses by expressing IFN antagonist proteins [4]. Although the specific mode of action of these factors can vary between different viruses, STATs

are major targets of many IFN antagonists, including those of RABV/lyssaviruses, dengue virus, influenza virus and paramyxoviruses [5], presumably due to the critical role of STATs in antiviral responses. The STAT-targeting activity of IFN antagonists is thus considered a determining factor in pathogenicity [3, 4, 6]. However, for many viruses, including lyssaviruses and paramyxoviruses, the genuine importance of STAT-targeting in infection and disease is unknown, primarily due to the fact that IFN antagonists are often multifunctional proteins with roles both in inhibiting immune signaling and in genome replication [3]. Thus, deletion or mutation of these proteins can impair viral growth/replication independently of effects on IFN antagonism [7].

The P-proteins are considered the major IFN antagonists of lyssaviruses due to their capacity to bind STATs via their C-terminal domain (CTD, residues 186-297 of RABV P-protein [8-10]), and cause nuclear exclusion of P-protein-STAT complexes via a strong export sequence within P-protein [11]; P-proteins can thereby inhibit activation of IFN-dependent reporter genes in protein expression studies [12]. Importantly, P-protein is multifunctional, having essential roles in genome replication as the polymerase cofactor through interaction of the CTD with viral N-protein [13, 14]. This suggests that the CTD has dual functions critical to infection, but the molecular details of P-protein-STAT interaction, including the location and constituent residues of the STAT-binding interface, and the structural mechanisms by which P-protein coordinates interactions with N- and STAT proteins, are unresolved. Importantly, no mutations have been identified that can inhibit STAT-binding without also inhibiting replication such that no viable mutant lyssavirus lacking STAT-binding function has been generated, preventing specific examination of the role of STAT antagonism in infection.

Here, we demonstrate that P-protein interactions with and antagonism of STATs is dependent on residues within a unique hydrophobic pocket (the "W-hole") of the CTD. Structural and mutagenic analysis indicated that P-protein thus utilizes functionally and spatially distinct interfaces in the CTD to coordinate interactions with N- and STAT proteins. Based on these findings, we introduced mutations into RABV to specifically inhibit STAT interaction, generating viable virus with growth kinetics indistinguishable from the parental strain in vitro, but which lacked IFN/STAT antagonist activity. This virus was highly sensitive to IFN and severely attenuated in vivo causing no lethality in mice, in contrast to the invariably lethal parental strain.

Methods:

Constructs, cells, transfections and infections. Constructs were generated by standard techniques (see Supplementary Information) or are described elsewhere [12, 15, 16].

Cells used were Cos-7, HEK293T, NA, Vero, SK-N-SH and BHK/T7-9 (see Supplementary Information for culture conditions). Transfections using Lipofectamine®2000 (Invitrogen) and infections were performed as previously [12, 17].

Luciferase assays. For IFNα-dependent signaling assays, Cos-7 cells cotransfected with pISRE-luc, pRL-TK, and pEGFP-C1 encoding P-proteins (6 h) were treated without or with 1000U/ml recombinant human IFNα (PBL Interferon Source) for 16 h before analysis in a dual luciferase assay, and calculation of relative luciferase activity as previously [12].

For minigenome assays, HEK293T cells transfected with pRVDI-luc, pC-RN, pC-RL, and pEGFP-C1 encoding P-proteins (48 h) were analyzed for firefly luciferase activity as above (see Supplementary Information).

qRT-PCR. HEK293T cells mock-transfected or transfected to express GFP-P-protein were treated 24 h later without or with 1000U/ml IFNα (8 h) to activate STAT-dependent signaling. To activate *IFNβ*, cells were cotransfected with Flag-RIG-I (24 h). Following activation, cells were lysed for total RNA extraction (RNeasy, Qiagen) and analysis by qRT-PCR using the SensiMix^{TM} SYBR Hi-ROX kit (Bioline) (Supplementary Information).

Immunoprecipitation (IP). IP used the GFP-Trap® system (Chromotek GmbH) with wash buffer supplemented with 1x PhosSTOP and 1x protease inhibitor, followed by immunoblotting (IB) analysis as previously [12] (see Supplementary Information).

Yeast-2-hybrid (**Y2H).** Two-hybrid analysis was performed using L40 yeast strain as previously [16] (see Supplementary Information).

Reverse genetics. Mutations were introduced to the CE-NiP-WT genome plasmid by overlap PCR as previously [17], and recombinant virus rescued in BHK/T7-9 cells. Viral stocks were prepared in NA cells, which are commonly used to prepare IFN-sensitive strains [18-20] and titers were determined by focus formation assay to calculate focus forming units (ffu)/ml as previously [17] (see Supplementary Information).

IFN sensitivity assays. Growth of virus in Vero cells inoculated at multiplicity of infection (MOI) 0.001 was analyzed daily by focus formation assay. In some assays, infected cells were cultured after 1 day post inoculation (dpi) with 500U/ml IFNα (see Supplementary Information.

Mouse infection. 12 6-week-old female ddY mice (Japan SLC Inc.) per group were inoculated intracerebrally (i.c.) with 0.03ml of diluent (mock) or diluent containing 10^4 ffu of virus. Mice were inspected for symptoms over 21 days (see Supplementary Information). To measure viral titer in brains, mice were euthanized at 5 dpi and brains homogenized for analysis by focus formation assays. Experiments were approved by the Committee for Animal Research and Welfare of Gifu University (Approval No. 10086).

Confocal laser scanning microscopy. SK-N-SH cells infected at MOI of 0.01 (18 h) were treated without or with IFNα (4,000U/ml, 0.5 h) before fixation and immunostaining for STAT1 and N-protein or Y701-phosphorylated STAT1 (pY-STAT1) and P-protein, followed by confocal microscopy analysis to calculate the nucleocytoplasmic fluorescence ratio (Fn/c) (mean Fn/c, n >30 cells) [12] (see Supplementary Information).

Statistical analysis. Unpaired two-tailed Student's t-test was performed using GraphPad Prism (5.0c).

Results:

STAT-binding and IFN antagonist activity of DUVV P-protein is reduced compared with that of RABV P-protein. We previously found that the P-proteins of several RABV strains, ABLV, and the distantly related MOKV interact with STATs and inhibit IFN-signaling to similar extents, indicating that this function is conserved across the genus [12]. DUVV causes lethal human disease, but is less pathogenic in mice than a WT RABV street strain [21]. To compare STAT antagonism by DUVV and RABV P-proteins, we expressed GFP-fused P-proteins in Cos-7 cells, and assessed effects on IFNα-signaling using a luciferase reporter gene assay [12]. IFNα-

signaling, indicated by induction of luciferase activity, was significantly ($p<0.0001$) reduced in cells expressing RABV P-WT compared with cells expressing a control P-protein lacking the C-terminal 30 residues (P-ΔC30) that does not bind STATs [10] (Figure 1A). Intriguingly, although DUVV P-WT also inhibited IFNα-signaling, it did so to a significantly ($p<0.0001$) lesser extent than RABV P-protein (Figure 1A).

To examine whether this difference related to differing STAT interaction, we performed IP of GFP-fused P-proteins from cell lysates used in the luciferase reporter assays and analyzed by IB. RABV P-protein interacts selectively with IFN-activated STATs, such that STAT1/2 are only precipitated from IFN-treated cells, while P-ΔC30 shows no interaction with STATs [12, 22] (Figure 1B). Importantly, although DUVV P-WT interacted with STAT1/2 in IFN-treated cells, it precipitated lower amounts of both compared with RABV P-WT (Figure 1B). Comparable results were obtained from luciferase reporter and IP assays using HEK293T cells (not shown). Thus, IFN antagonism by DUVV P-protein was impaired compared with that of RABV P-protein, and this correlated with differing interaction with STATs.

W-hole residues W265 and M287 are essential for STAT1/2-binding. Structural analysis of the RABV and MOKV P-protein CTDs has identified a conserved fold forming a "half-pear" structure with two putative molecular interfaces: a positive patch on the round face, implicated in N-protein-binding, and the W-hole on the flat face, of unknown function [13, 14, 23] (Figures 2A, B).

Analysis of P-protein sequences from 120 field isolates of RABV, DUVV, and 12 other lyssaviruses indicated that positive patch residues K211, K212, K214 and R260 are 100% conserved, and W-hole residues C261 and M287 show nearly 100% identity (not shown), consistent with important functions. Interestingly however, W265 of RABV P-protein is substituted for glycine in DUVV. To examine the potential role of

this substitution in P-protein-STAT interaction, we substituted W265 for glycine in RABV P-protein (P-W265G, denoted as *W* in figures), identifying substantially impaired STAT1/2 interaction and antagonism in IP and luciferase reporter assays (Figure 2C).

To further assess the role of the W-hole, we selected for mutation the residue M287, which is 100% conserved among lyssavirus P-proteins except those of MOKV and Ikoma virus where it is substituted for isoleucine. STAT-binding and antagonism by the P-protein of MOKV is comparable to those of RABV and ABLV [12], suggesting that the methionine sulphur atom is not critical, but that size/structure of the residue might be important. We thus mutated M287 of DUVV and RABV P-proteins to valine (P-M287V, denoted as *M* in figures), thereby retaining hydrophobicity at this position, but introducing a shorter, bulkier residue. This substantially reduced IFNα antagonism and STAT-binding by RABV P-protein in IP and luciferase reporter assays, and entirely prevented these functions in DUVV P-protein (Figure 2C), perhaps relating to a requirement for conformational flexibility in STAT-binding that is restricted due to the presence of the branched β-carbon atom in the side chain of valine. This suggested that combined mutation of W265G and M287V would strongly impact STAT-binding/antagonism, and this was confirmed in IP and luciferase reporter assays using Cos-7 and HEK293T cells expressing RABV P-protein containing both mutations (P-W265G/M287V, denoted as *W/M* in figures) (Figure 2D, not shown). In addition qRT-PCR analysis indicated that W265G/M287V mutation entirely prevents P-protein antagonism of IFN-dependent activation of the ISGs *ISG15* and *MxA* (Figure 3), which have been implicated in negative strand RNA virus infection [8, 24, 25]. The difference observed between P-WT and P-W265G/M287V was reproduced in 3 separate qRT-PCR assays.

P-protein expression or RABV infection also inhibits dephosphorylation of IFN-activated pY-STAT1, potentially by inhibiting interaction with nuclear phosphatases, and thereby impairing STAT-recycling [22]. IB analysis of Cos-7 cell lysates revealed that pY-STAT1 was clearly present in RABV P-WT-expressing cells at 16 h post-IFN treatment, as expected [12], but was undetectable in cells expressing P-ΔC30 or P-W265G/M287V (Figure S1A), consistent with defective STAT1 interaction. Thus, W265G/M287V mutation strongly impairs P-protein interaction with and functional modification of STATs.

W265G/M287V mutation does not impair P-protein functions in genome replication or antagonism of IFN induction. Since the W-hole and N-protein-binding sites are spatially distinct in the CTD (Figures 2A, B) [14, 23], we hypothesized that STAT-binding/antagonism and N-binding/replication functions of P-protein might be separable. Consistent with this, IP assays using Cos-7 cells coexpressing GFP-fused CTD regions of WT or mutant RABV P-protein with mCherry-fused N-protein revealed that N-protein interacts with P-WT, P-W265G, P-M287V, and P-W265G/M287V CTDs, but not with a control CTD in which the N-binding site is mutated (P-K214A/R260A, denoted as *K/R* in figures) (Figure 4A). Comparable results were obtained using HEK293T cells (not shown) as well as by Y2H analysis (Figure 4B). P-ΔC30, previously used as a STAT-binding deficient P-protein, lacks N-binding function through the CTD [26], indicative of broad effects due to deletion of 30 residues from the globular domain [14]. Thus, W265G/M287V mutation appears to affect STAT-binding selectively.

To confirm that P-W265G/M287V is functional in genome replication, we used a minigenome system encoding a luciferase reporter (Supplementary Information). RABV P-W265G, P-M287V and P-W265G/M287V induced luciferase expression to

the same extent as P-WT, indicative of unimpaired polymerase cofactor activity; as expected P-K214A/R260A and P-ΔC30 lacked this function (Figure 4C). Together these data indicated that P-protein interactions with N-protein and STATs are separable, and likely to be mediated by discrete independent interfaces (the positive patch and W-hole, respectively) on opposite faces of the CTD (Figures 2A, B). Consistent with this, although K214A/R260A mutations prevented P-N-protein interaction, they did not prevent P-protein-STAT-binding (Figure S1B).

In addition to roles in STAT antagonism and genome replication, P-protein can inhibit viral induction of IFNβ [27]. To examine potential effects thereon of W265G/M287V mutation, we used RIG-I overexpression to induce *IFNβ* expression [15, 28, 29], detecting clear induction by qRT-PCR (Figure 4D). This was strongly inhibited by P-WT and, importantly, P-W265G/M287V caused inhibition to the same extent (Figure 4D). Thus, the effects of the mutations appear to be highly specific to antagonism of STAT1/2.

RABV carrying W265G and M287V mutations is viable but highly sensitive to IFN. To examine the effect of W265G/M287V mutation in RABV, we used the CE-NiP strain (hereon referred to as CE-NiP-WT), which we showed can efficiently bind STAT1 via the P-protein and inhibit STAT1/2-dependent signaling, and causes neurological symptoms and death in infected mice [17]. Introduction of W265G/M287V mutations generated the CE-NiP-STAT(-) virus, which was clearly viable, producing titers of $>10^7$ ffu/ml in NA cells. RT-PCR/sequencing confirmed that the rescued virus retained the W265G/M287V mutations.

To compare the growth kinetics of CE-NiP-STAT(-) and CE-NiP-WT, we infected Vero cells, which do not produce IFN [30], and monitored growth by focus formation assays, with results indicating identical growth (Figure 5A). Importantly, however, in

cells treated with 500U/ml IFNα for 2 days, growth of CE-NiP-STAT(-) was substantially impaired compared with CE-NiP-WT (a decrease of ca. 3 log versus ca. 1 log, respectively), indicative of greatly increased IFN sensitivity of the mutant strain (Figure 5B).

To examine effects of the mutations on viral inhibition of STAT responses, we infected human neuroblastoma SK-N-SH cells and treated without or with IFNα (4000U/ml, 0.5 h) before fixation and immunostaining for N-protein and STAT1 (Figure 6A) or P-protein and pY-STAT1 (not shown), and analysis by confocal microscopy. Consistent with conservation of N-binding and replication function in P-W265G/M287V protein, viral N- and P-antigen was clearly detectable in cells infected by CE-NiP-WT and CE-NiP-STAT(-), and showed a typical distribution, with accumulation in cytoplasmic Negri bodies (the major sites of genome transcription/replication [31]) (Figure 6A, not shown). Calculation of the nucleocytoplasmic fluorescence ratio for P-protein [12] also indicated that its nucleocytoplasmic localization was equivalent in CE-NiP-WT and CE-NiP-STAT(-)-infected cells (not shown), demonstrating that the mutations do not affect nuclear export of P-protein, which was previously implicated in STAT antagonist function [17]. By contrast, STAT1 localization differed between IFN-treated cells infected with CE-NiP-WT and CE-NiP-STAT(-), with clearly greater levels of nuclear STAT1 in the latter (Figure 6A, not shown). Determination of the nucleocytoplasmic fluorescence ratio confirmed significantly ($p<0.0001$) greater localization of IFN-activated STAT1 to the nucleus of CE-NiP-STAT(-)-infected cells compared with CE-NiP-WT-infected cells (Figure 6B, not shown). Importantly, the nuclear accumulation of IFN-activated STAT1 in CE-NiP-STAT(-)-infected cells was not

different to that in mock-infected cells, consistent with a strong defect in P-protein-STAT complex formation.

CE-NiP-STAT(-) virus is strongly attenuated in vivo. To examine viral pathogenicity, we i.c. inoculated 12 ddY mice with 10^4 ffu of CE-NiP-WT or CE-NiP-STAT(-), and monitored symptoms over 21 dpi (Figures 7A, B). CE-NiP-WT infection caused marked weight loss and severe neurological symptoms in all mice by 7 dpi (Figures 7A, B), similar to previous observations [32], and all mice succumbed to infection or reached a non-responsive end-point between 6 and 13 dpi (Figure 7A). By contrast, the only symptoms of CE-NiP-STAT(-) infection were temporary weight loss (11/12 mice) and mild ataxia in one mouse (Figures 7A, B). No neurological symptoms were observed by 21 dpi, and weight loss/ataxia was no longer evident by 18 dpi (Figures 7A, B), indicating recovery from infection. Comparable results were obtained in two independent assays (Movie S1). Importantly, the infectious virus load of mouse brains infected with CE-NiP-STAT(-) (5 dpi) was 10^3-10^6-fold lower than that of mouse brains infected with CE-NiP-WT (Figure 7C), indicating that the different symptoms relate to the levels of virus in target tissues of the central nervous system (CNS).

Discussion: In this study, we investigated the mechanism by which P-protein coordinates multiple interactions important to roles in the basic viral life cycle and in viral immune evasion, and developed the first mutant lyssavirus specifically deficient for interaction with STATs. Using this virus, we showed that P-protein-STAT1/2 interaction is critical to pathogenicity, identifying the P-protein-STAT complex as a key pathogen-host interface in the development of rabies. Importantly, the finding that P-WT but not P-W265G/M287V can inhibit IFNα-dependent expression of ISGs, but

that both proteins mediate genome replication and antagonism of *IFNβ* induction, enabled delineation of the specific importance of P-protein targeting of STATs in disease, with the finding that W265G/M287V mutation profoundly impairs RABV pathogenicity in vivo indicative of a major contribution. Notably, the fact that CE-NiP-STAT(-) caused no major neurological symptoms in mice in spite of inoculation into the brain indicates a critical role for P-STAT interaction in infection of the CNS, consistent with the importance of IFN-mediated innate immunity in these tissues, from which cells of the adaptive response are excluded by the blood-brain barrier [33, 34]. This is further supported by the observation of a > 3 log difference in infectious virus load of WT and STAT(-) virus in the CNS within 5 dpi. Thus our data support a central role for P-protein-STAT interactions in the principal target organs of lyssavirus infection. However, we cannot discount the possibility that other as yet unidentified functions of P-protein might be affected by W265G/M287V mutations, and that this might contribute to the reduced pathogenicity. Future analysis of infection of IFNAR-knockout mice and mice deficient for specific STATs will provide further insights into the precise role of P-protein-STAT targeting in pathogenicity.

In common with other viruses that use P-gene products for IFN antagonism, the role of lyssavirus-STAT interaction in disease has proven elusive [35, 36], largely because of the complex roles of P-gene products in both IFN antagonism and genome replication. As a result, previously identified mutations that inhibit STAT-binding (e.g. RABV P-ΔC30) have also prevented the formation of a functional replication complex (Figure 4C), precluding the generation of fully viable virus deficient for STAT interaction. Point mutations that inhibit STAT-binding by the P-gene-encoded V-protein of measles virus have been described, and were used to generate mutant

virus that showed moderately reduced disease symptoms, but also showed defective growth in IFN-deficient cells, indicating effects distinct from IFN antagonism [7]. Studies of Nipah virus P/V/W-proteins also suggested that genome replication and STAT-binding/mislocalization functions are separable in vitro, but effects of mutations on antagonism of STAT-signaling, viral IFN resistance, and disease progression are yet to be reported [37]. Thus the present study is to our knowledge the first to separate STAT antagonism and replication functions of a P-gene product, with significance to understanding of the mechanisms of infection by lyssaviruses and paramyxoviruses, and potential significance to analogous multifunctional STAT antagonists, such as Ebola virus VP35, dengue and West Nile virus NS5, and hepatitis C virus NS5A [3, 38, 39] for which the importance of IFN antagonist function in vivo is yet to be demonstrated.

Critical to this study was the finding that key residues for STAT-binding reside within the P-protein W-hole enabling direct analysis of the localization of interfaces for STAT and N-protein interaction in the globular CTD structure. This provided indications that these sites are spatially and functionally separable, a finding which has important implications for our understanding of basic lyssavirus biology. In particular, it has not previously been understood how P-protein could efficiently mediate IFN/STAT-antagonism, as most P-protein is likely to be engaged in P-N complexes in infected cells, where N is produced in excess over P [40]. Our findings suggest that P-protein might form interactions with N- and STAT proteins simultaneously through interfaces on opposite sides of the CTD, such that STAT antagonism would not be restricted to limited amounts of free P-protein, but could also involve P-N complexes.

Rabies remains a major threat to human and animal health worldwide due to the absence of effective therapeutics, and the limitations of current inactivated vaccines. The potential of targeting viral IFN antagonism for the development of vaccines and antivirals is well appreciated [3, 4, 41], and the data in this study now provide evidence that IFN antagonist-STAT interactions specifically represent viable targets. The identification of novel attenuating mutations in P-protein, and of the W-hole as the interface of P-STAT interaction, is thus of potential significance to efforts to develop new attenuated lyssavirus vaccine strains and novel therapeutics for currently incurable rabies disease. Future work will include analysis of the effect of these mutations in live RABV vaccine strains to examine both induction of immune responses, including ISG expression, and establishment of protective immunity.

References:

1. Knobel DL, Cleaveland S, Coleman PG, et al. Re-evaluating the burden of rabies in Africa and Asia. Bull World Health Organ **2005**; 83:360-8.

2. Evans JS, Horton DL, Easton AJ, Fooks AR, Banyard AC. Rabies virus vaccines: Is there a need for a pan-lyssavirus vaccine? Vaccine **2012**; 30:7447-54.

3. Randall RE, Goodbourn S. Interferons and viruses: an interplay between induction, signalling, antiviral responses and virus countermeasures. J Gen Virol **2008**; 89:1-47.

4. Versteeg GA, Garcia-Sastre A. Viral tricks to grid-lock the type I interferon system. Curr Opin Microbiol **2010**; 13:508-16.

5. Najjar I, Fagard R. STAT1 and pathogens, not a friendly relationship. Biochimie **2010**; 92:425-44.

6. Oksayan S, Ito N, Moseley G, Blondel D. Subcellular trafficking in rhabdovirus infection and immune evasion: a novel target for therapeutics. Infect Disord Drug Targets **2012**; 12:38-58.

7. Devaux P, Hudacek AW, Hodge G, Reyes-Del Valle J, McChesney MB, Cattaneo R. A recombinant measles virus unable to antagonize STAT1 function cannot control inflammation and is attenuated in rhesus monkeys. J Virol **2011**; 85:348-56.

8. Brzozka K, Finke S, Conzelmann KK. Identification of the rabies virus alpha/beta interferon antagonist: phosphoprotein P interferes with phosphorylation of interferon regulatory factor 3. J Virol **2005**; 79:7673-81.

9. Lieu KG, Brice A, Wiltzer L, et al. The Rabies Virus Interferon Antagonist P Protein Interacts with Activated STAT3 and Inhibits Gp130 Receptor Signaling. J Virol **2013**; 87:8261-5.

10. Vidy A, Chelbi-Alix M, Blondel D. Rabies virus P protein interacts with STAT1 and inhibits interferon signal transduction pathways. J Virol **2005**; 79:14411-20.

11. Pasdeloup D, Poisson N, Raux H, Gaudin Y, Ruigrok RW, Blondel D. Nucleocytoplasmic shuttling of the rabies virus P protein requires a nuclear localization signal and a CRM1-dependent nuclear export signal. Virology **2005**; 334:284-93.

12. Wiltzer L, Larrous F, Oksayan S, et al. Conservation of a Unique Mechanism of Immune Evasion across the Lyssavirus Genus. J Virol **2012**; 86:10194-9.

13. Assenberg R, Delmas O, Ren J, et al. Structure of the nucleoprotein binding domain of Mokola virus phosphoprotein. J Virol **2010**; 84:1089-96.

14. Mavrakis M, McCarthy AA, Roche S, Blondel D, Ruigrok RW. Structure and function of the C-terminal domain of the polymerase cofactor of rabies virus. J Mol Biol **2004**; 343:819-31.

15. Rothenfusser S, Goutagny N, DiPerna G, et al. The RNA helicase Lgp2 inhibits TLR-independent sensing of viral replication by retinoic acid-inducible gene-I. J Immunol **2005**; 175:5260-8.

16. Raux H, Flamand A, Blondel D. Interaction of the rabies virus P protein with the LC8 dynein light chain. J Virol **2000**; 74:10212-6.

17. Ito N, Moseley GW, Blondel D, et al. Role of interferon antagonist activity of rabies virus phosphoprotein in viral pathogenicity. J Virol **2010**; 84:6699-710.

18. Schubert D, Humphreys S, Baroni C, Cohn M. In vitro differentiation of a mouse neuroblastoma. Proc Natl Acad Sci U S A **1969**; 64:316-23.

19. Shimizu K, Ito N, Sugiyama M, Minamoto N. Sensitivity of rabies virus to type I interferon is determined by the phosphoprotein gene. Microbiol Immunol **2006**; 50:975-8.

20. Masatani T, Ito N, Ito Y, et al. Importance of rabies virus nucleoprotein in viral evasion of interferon response in the brain. Microbiol Immunol **2013**; 57:511-7.

21. Koraka P, Martina BE, Roose JM, et al. In vitro and in vivo isolation and characterization of duvenhage virus. PLoS Pathog **2012**; 8:e1002682.

22. Brzozka K, Finke S, Conzelmann KK. Inhibition of interferon signaling by rabies virus phosphoprotein P: activation-dependent binding of STAT1 and STAT2. J Virol **2006**; 80:2675-83.

23. Assenberg R, Delmas O, Morin B, et al. Genomics and structure/function studies of Rhabdoviridae proteins involved in replication and transcription. Antiviral Res **2010**; 87:149-61.

24. Niu X, Tang L, Tseggai T, Guo Y, Fu ZF. Wild-type rabies virus phosphoprotein is associated with viral sensitivity to type I interferon treatment. Arch Virol **2013**; 158:2297-305.

25. Leroy M, Baise E, Pire G, Gerardin J, Desmecht D. Resistance of paramyxoviridae to type I interferon-induced Bos taurus Mx1 dynamin. J Interferon Cytokine Res **2005**; 25:192-201.

26. Chenik M, Chebli K, Gaudin Y, Blondel D. In vivo interaction of rabies virus phosphoprotein (P) and nucleoprotein (N): existence of two N-binding sites on P protein. J Gen Virol **1994**; 75 (Pt 11):2889-96.

27. Rieder M, Brzozka K, Pfaller CK, Cox JH, Stitz L, Conzelmann KK. Genetic dissection of interferon-antagonistic functions of rabies virus phosphoprotein: inhibition of interferon regulatory factor 3 activation is important for pathogenicity. J Virol **2011**; 85:842-52.

28. Biacchesi S, LeBerre M, Lamoureux A, et al. Mitochondrial antiviral signaling protein plays a major role in induction of the fish innate immune response against RNA and DNA viruses. J Virol **2009**; 83:7815-27.

29. Yoneyama M, Kikuchi M, Natsukawa T, et al. The RNA helicase RIG-I has an essential function in double-stranded RNA-induced innate antiviral responses. Nat Immunol **2004**; 5:730-7.

30. Desmyter J, Melnick JL, Rawls WE. Defectiveness of interferon production and of rubella virus interference in a line of African green monkey kidney cells (Vero). J Virol **1968**; 2:955-61.

31. Lahaye X, Vidy A, Pomier C, et al. Functional characterization of Negri bodies (NBs) in rabies virus-infected cells: Evidence that NBs are sites of viral transcription and replication. J Virol **2009**; 83:7948-58.

32. Shimizu K, Ito N, Mita T, et al. Involvement of nucleoprotein, phosphoprotein, and matrix protein genes of rabies virus in virulence for adult mice. Virus Res **2007**; 123:154-60.

33. Sorgeloos F, Kreit M, Hermant P, Lardinois C, Michiels T. Antiviral type I and type III interferon responses in the central nervous system. Viruses **2013**; 5:834-57.

34. Griffin DE. Immune responses to RNA-virus infections of the CNS. Nat Rev Immunol **2003**; 3:493-502.

35. Audsley MD, Moseley GW. Paramyxovirus evasion of innate immunity: Diverse strategies for common targets. World J Virol **2013**; 2:14.

36. Ramachandran A, Horvath CM. Paramyxovirus disruption of interferon signal transduction: STATus report. J Interferon Cytokine Res **2009**; 29:531-7.

37. Ciancanelli MJ, Volchkova VA, Shaw ML, Volchkov VE, Basler CF. Nipah virus sequesters inactive STAT1 in the nucleus via a P gene-encoded mechanism. J Virol **2009**; 83:7828-41.

38. Leung DW, Prins KC, Borek DM, et al. Structural basis for dsRNA recognition and interferon antagonism by Ebola VP35. Nat Struct Mol Biol **2010**; 17:165-72.

39. Ye J, Zhu B, Fu ZF, Chen H, Cao S. Immune evasion strategies of flaviviruses. Vaccine **2013**; 31:461-71.

40. Wunner WH, Conzelmann KK. Rabies Virus. In: Jackson AC, ed. Rabies: Scientific Basis of the Disease and its Management. 3 ed: Academic Press, Elsevier, **2013**.

41. Richt JA, Garcia-Sastre A. Attenuated influenza virus vaccines with modified NS1 proteins. Curr Top Microbiol Immunol **2009**; 333:177-95.

42. Moseley GW, Lahaye X, Roth DM, et al. Dual modes of rabies P-protein association with microtubules: a novel strategy to suppress the antiviral response. J Cell Sci **2009**; 122:3652-62.

43. Moseley GW, Roth DM, DeJesus MA, et al. Dynein light chain association sequences can facilitate nuclear protein import. Mol Biol Cell **2007**; 18:3204-13.

44. Oksayan S, Wiltzer L, Rowe CL, Blondel D, Jans DA, Moseley GW. A novel nuclear trafficking module regulates the nucleocytoplasmic localization of the rabies virus interferon antagonist, P protein. J Biol Chem **2012**; 287:28112-21.

Figure Legends:

Figure 1. Interaction with STATs and antagonism of STAT-signaling by DUVV P-protein is reduced compared with RABV P-protein. (A) Cos-7 cells transfected to express the indicated GFP-fused P-proteins and with plasmids for the IFNα-dependent luciferase reporter assay were treated 6 h post-transfection with IFNα (1000U/ml, 16 h) before analysis of luciferase activity [12] (upper panel). Values for normalized luciferase activity are shown relative to those obtained for IFNα-treated P-ΔC30-expressing samples (mean relative luciferase activity ± SEM, n=4; data are from a single assay representative of 3 independent assays); **, $p \leq 0.01$; ****, $p \leq 0.0001$. Cell lysates from assays corresponding to those shown in the histogram were also analyzed by IB for P-protein (lower panel). (B) Cell lysates of IFNα-treated samples from luciferase assays described in A were subjected to IP for GFP-fused P-protein, followed by IB analysis of lysate (input) and precipitate (IP) for STAT1, STAT2 and GFP-P-protein (blot is representative of 3 independent assays).

Figure 2. W-hole residues 265 and 287 are critical to STAT antagonism by P-protein. Surface representations showing the side (A) and flat face (B) of the RABV P-protein CTD (residues 186-297, PDB file 1VYI) [23] with W-hole residues W265, M287 and C261 in red and residues K211, K214 and R260 of the positive patch (corresponding to the N-binding site) in blue. (C, D) Luciferase reporter assays (upper panels) and IP analysis of corresponding samples (lower panels) from IFNα-treated (1000U/ml, 16 h) Cos-7 cells expressing the indicated GFP-fused P-proteins were performed as described in the legend to Figure 1 (mean relative luciferase activity ± SEM, n=4; data are from a single assay representative of 3 independent assays; P-M287V, M; P-W265G, W; P-W265G/M287V, W/M); ns, non-significant; **, $p \leq 0.01$;

*** p≤0.001; ****, p≤0.0001. The Western blots are representative of 3 independent assays.

Figure 3. P-protein-mediated inhibition of ISG expression is prevented by mutations of residues 265 and 287. HEK293T cells were mock-transfected or transfected to express the indicated GFP-fused P-proteins before treatment without or with IFNα (1000U/ml, 8 h) and qRT-PCR analysis of *ISG15* and *MxA* transcripts (upper panel). Data show mean relative mRNA expression normalized to that of *GAPDH* (mean ± SEM, n=3; data from 3 assays); *, p≤0.05; **, p≤0.01; ***, p≤0.001. Cell lysates from samples corresponding to those shown in the histogram were analyzed by IB (lower panel); tub, tubulin.

Figure 4. W-hole mutation W265G/M287V does not impair polymerase cofactor function or antagonism of IFNβ induction by P-protein. (A) Cos-7 cells cotransfected to express GFP-fused CTD regions of the indicated P-proteins with mCherry-fused N-protein were subjected to IP for GFP and IB analysis; P-K214A/R260A, K/R. (B) Yeast cells were transformed with pLex plasmid encoding CTD regions of the indicated P-proteins and pGAD plasmid encoding N-protein (N) or empty pGAD (0) for analysis in a Y2H assay. P-N-protein interaction is indicated by the presence of blue colonies. (C) HEK293T cells cotransfected to express RABV N-, L-, and the indicated GFP-P-proteins, and with pRVDI-luc minigenome plasmid were analyzed for luciferase activity 48 h later (mean relative luciferase activity ± SEM, n=6; data are from a single assay representative of 2 independent assays); ns, non-significant; ****, p<0.0001. (D) HEK293T cells cotransfected to express Flag-tagged RIG-I without (mock) or with the indicated GFP-fused P-protein were analyzed by qRT-PCR for *IFNβ* transcript 24 h later. Data show mean relative expression of *IFNβ* normalized to that of *GAPDH* (mean ± SEM, n=4; data from 2

assays); ns, non-significant; ****, p≤0.0001; con, no RIG-I control. Cell lysates from samples corresponding to those used for qRT-PCR were analyzed by IB for GFP-fused P-protein and Flag-RIG-I (lower panel).

Figure 5. CE-NiP-STAT(-) virus is more sensitive to IFN than CE-NiP-WT virus. (A) Vero cells were infected with CE-NiP-WT or CE-NiP-STAT(-) viruses (MOI of 0.001) and titers (ffu/ml) were determined every 24 h for 4 dpi by focus formation assays (data are from a single assay representative of 3 independent assays). (B) Vero cells infected as in A were treated at 1 dpi without or with 500U/ml IFNα and titers were determined at 3 dpi (data are from a single assay representative of 2 independent assays).

Figure 6. CE-NiP-STAT(-) virus cannot prevent IFNα-induced nuclear accumulation of STAT1. (A) SK-N-SH cells were mock-infected or infected with CE-NiP-WT or CE-NiP-STAT(-) (MOI of 0.01, 18 h) and treated without or with 4000U/ml IFNα for 0.5 h before fixation, immunostaining using anti-N-protein and anti-STAT1 antibodies with Alexa-568- and Alexa-488-conjugated secondary antibodies, and analysis by confocal microscopy. Open arrowheads indicate N-positive cells; filled white arrowheads in STAT1-immunostained cells indicate the nucleus. (B) Confocal microscopic images such as those shown in A were used to determine the nucleocytoplasmic fluorescence ratio (Fn/c) for STAT1 as previously [42-44] (mean ± SEM, n>30 cells; data are from a single assay representative of 2 independent assays); ****, p≤0.0001.

Figure 7. CE-NiP-STAT(-) virus is strongly attenuated in vivo compared with CE-NiP-WT. (A) 10^4 ffu of the indicated virus was inoculated i.c. into mice (12 per group) and disease symptoms were monitored for 21 dpi. All CE-NiP-WT-infected mice succumbed to infection or reached a non-responsive end-point and were

sacrificed by 12 dpi, but no lethality was observed for mock- or CE-NiP-STAT(-)-infected mice. (B) Mean body weight changes of the infected mice described in A are shown. (C) Viral titers in brain emulsions (ffu/g) from 5 mice infected with the indicated viruses were measured at 5 dpi by focus formation assays.

Figure 1
Click here to download high resolution image

Figure 1

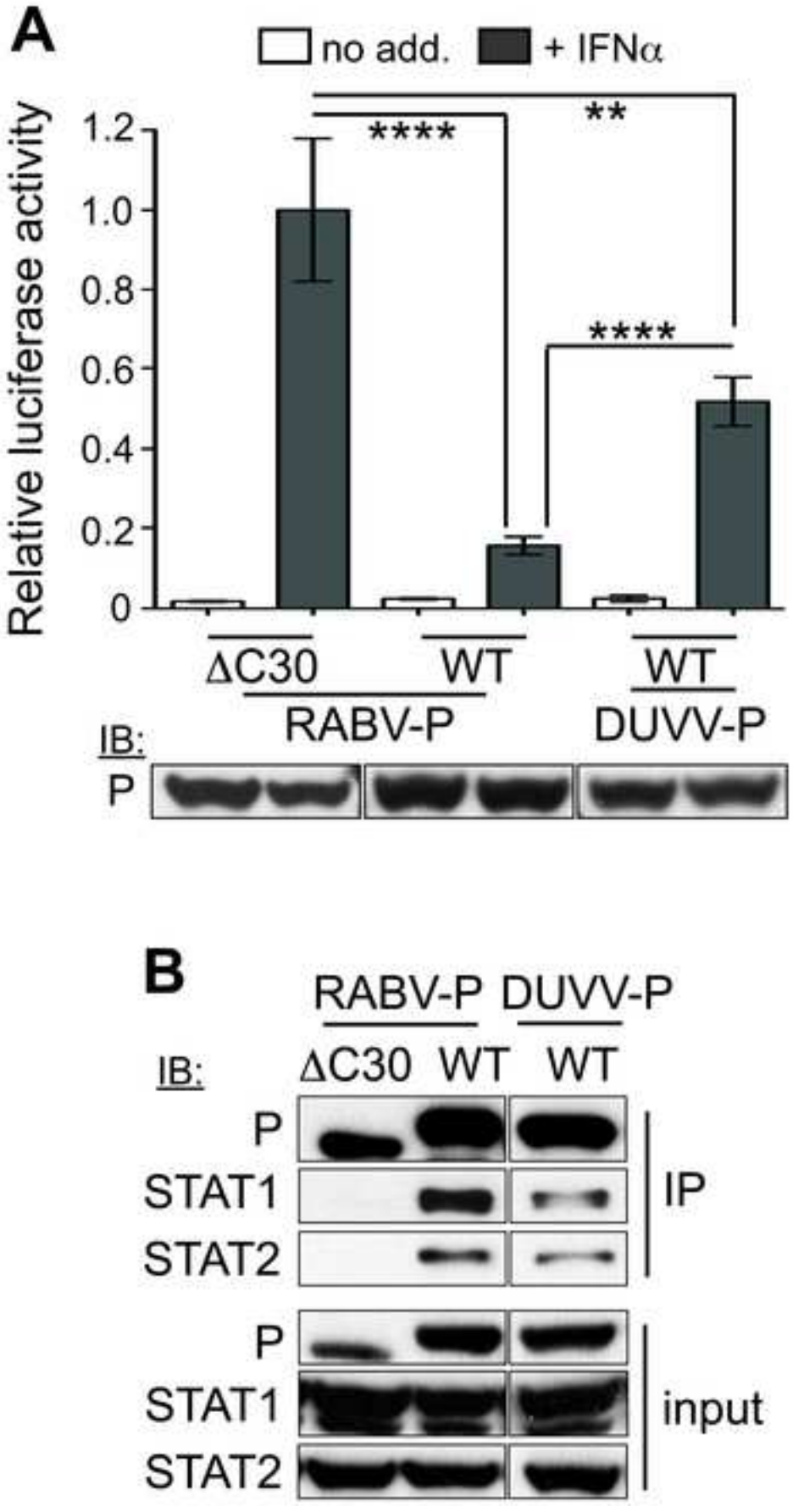

Figure 2
Click here to download high resolution image

Figure 2

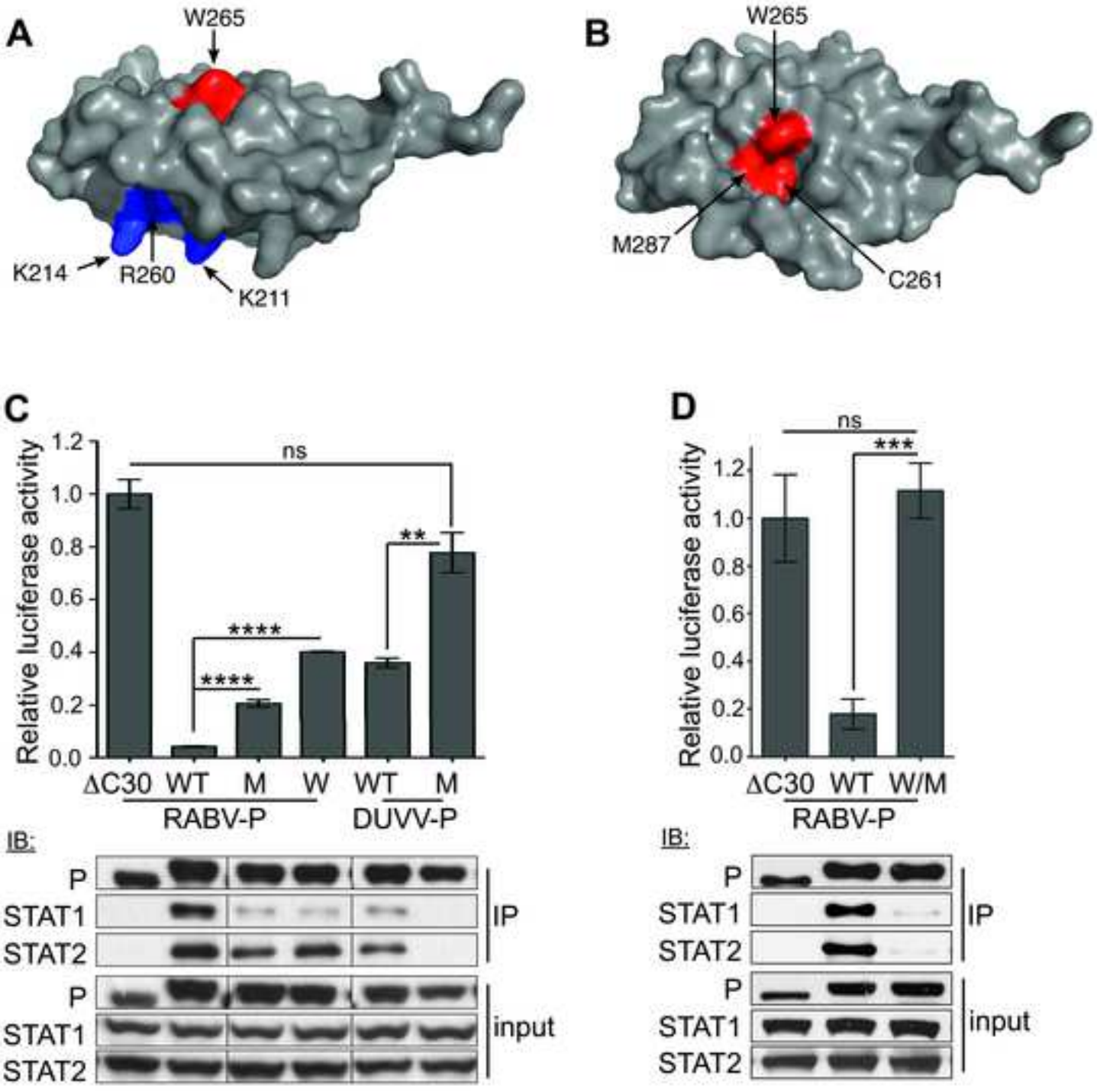

Figure 3
Click here to download high resolution image

Figure 3

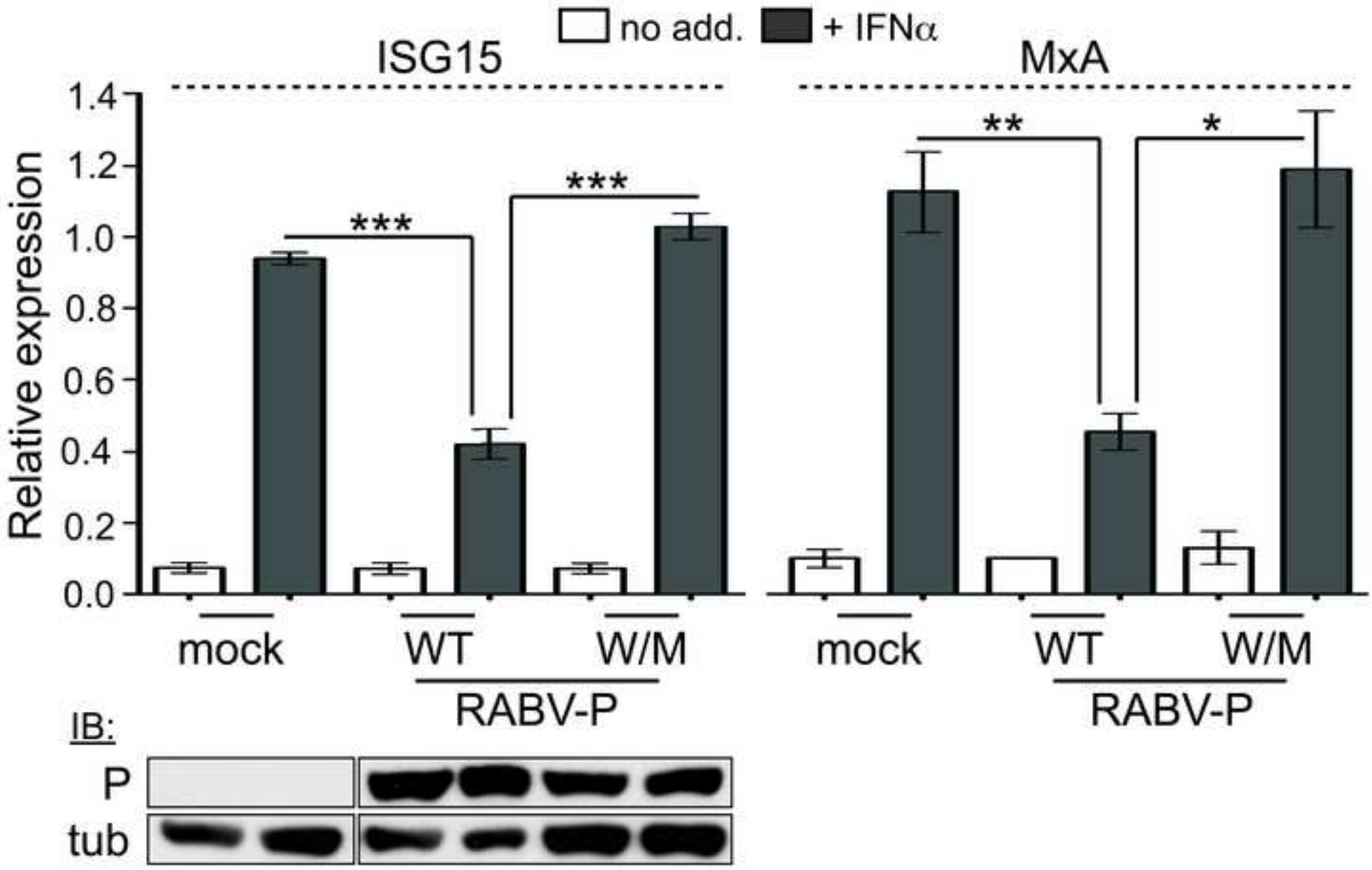

Figure 4
Click here to download high resolution image

Figure 4

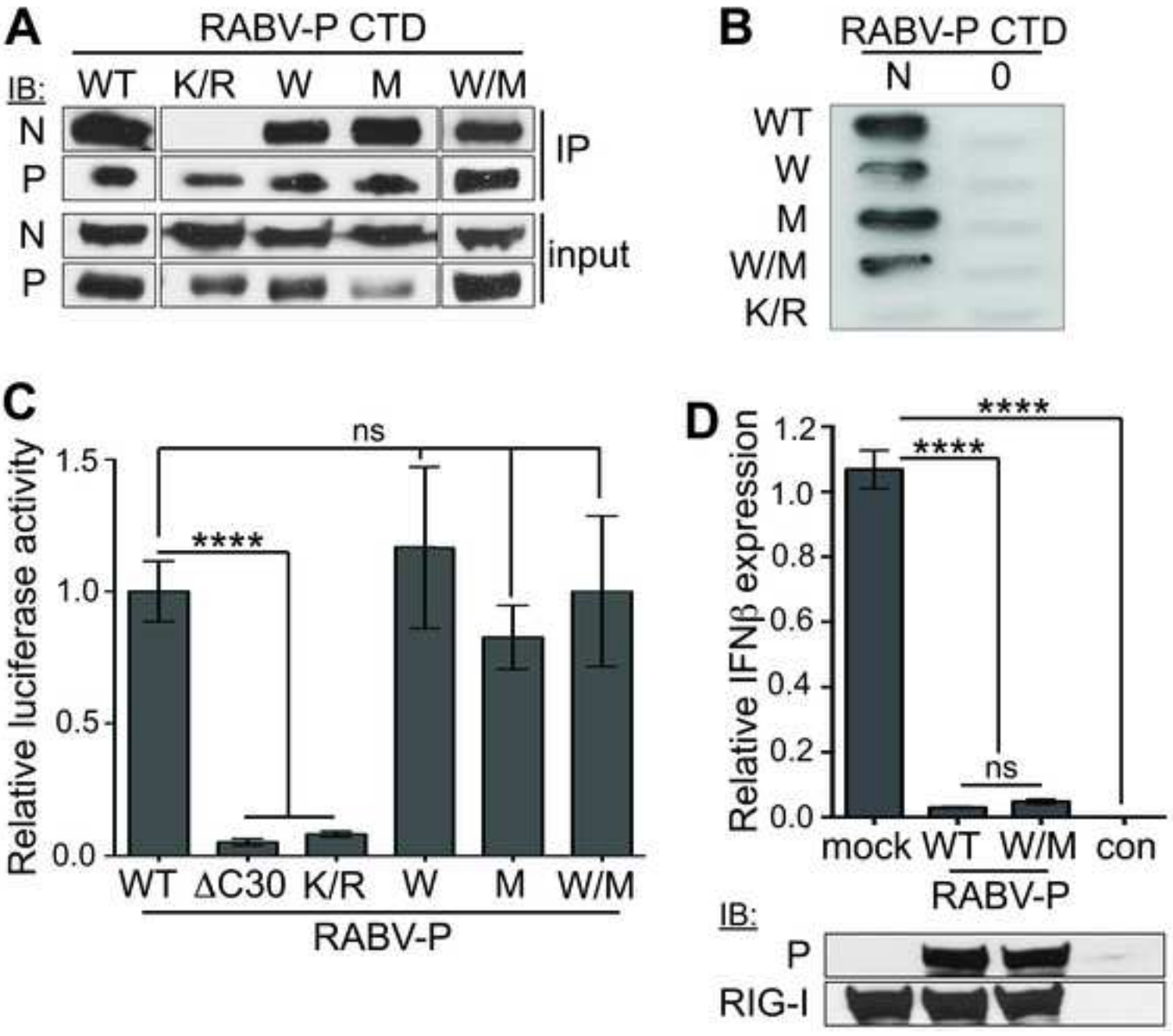

Figure 5
Click here to download high resolution image

Figure 5

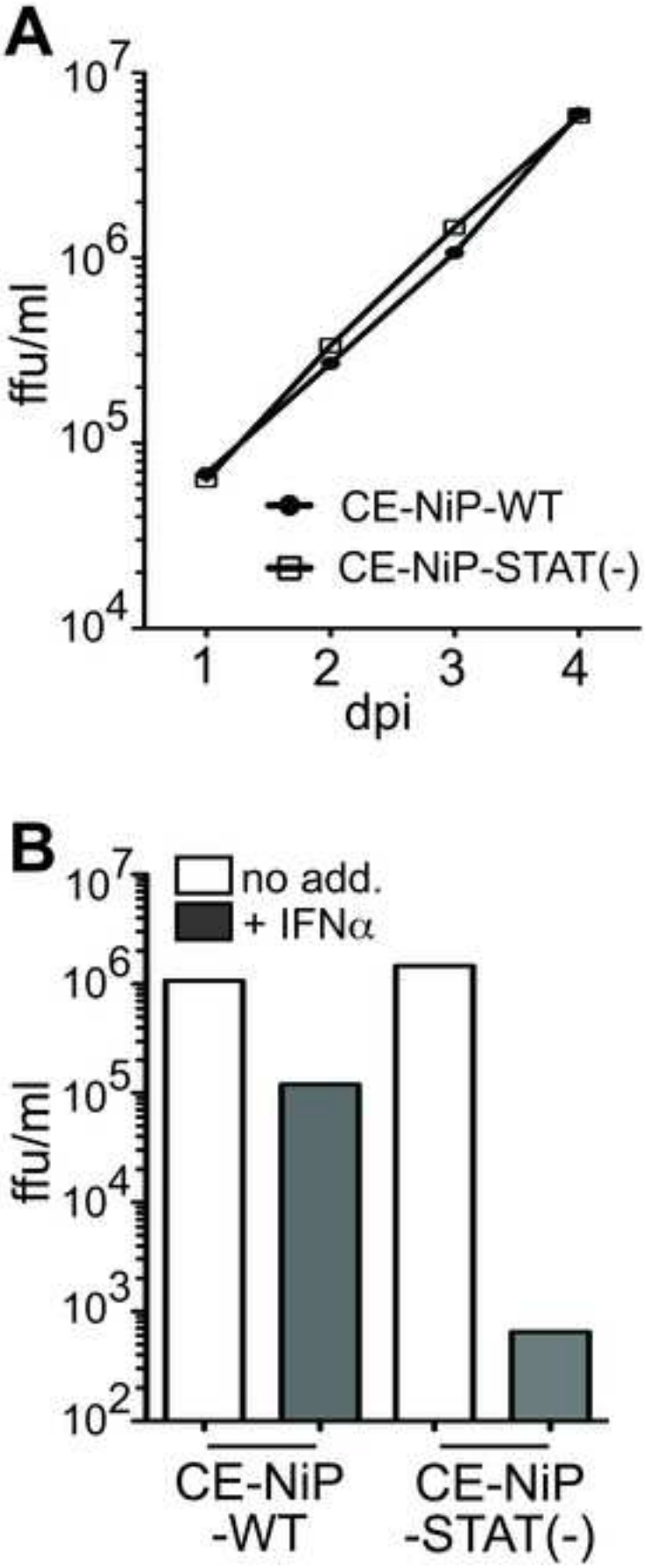

Figure 6
Click here to download high resolution image

Figure 6

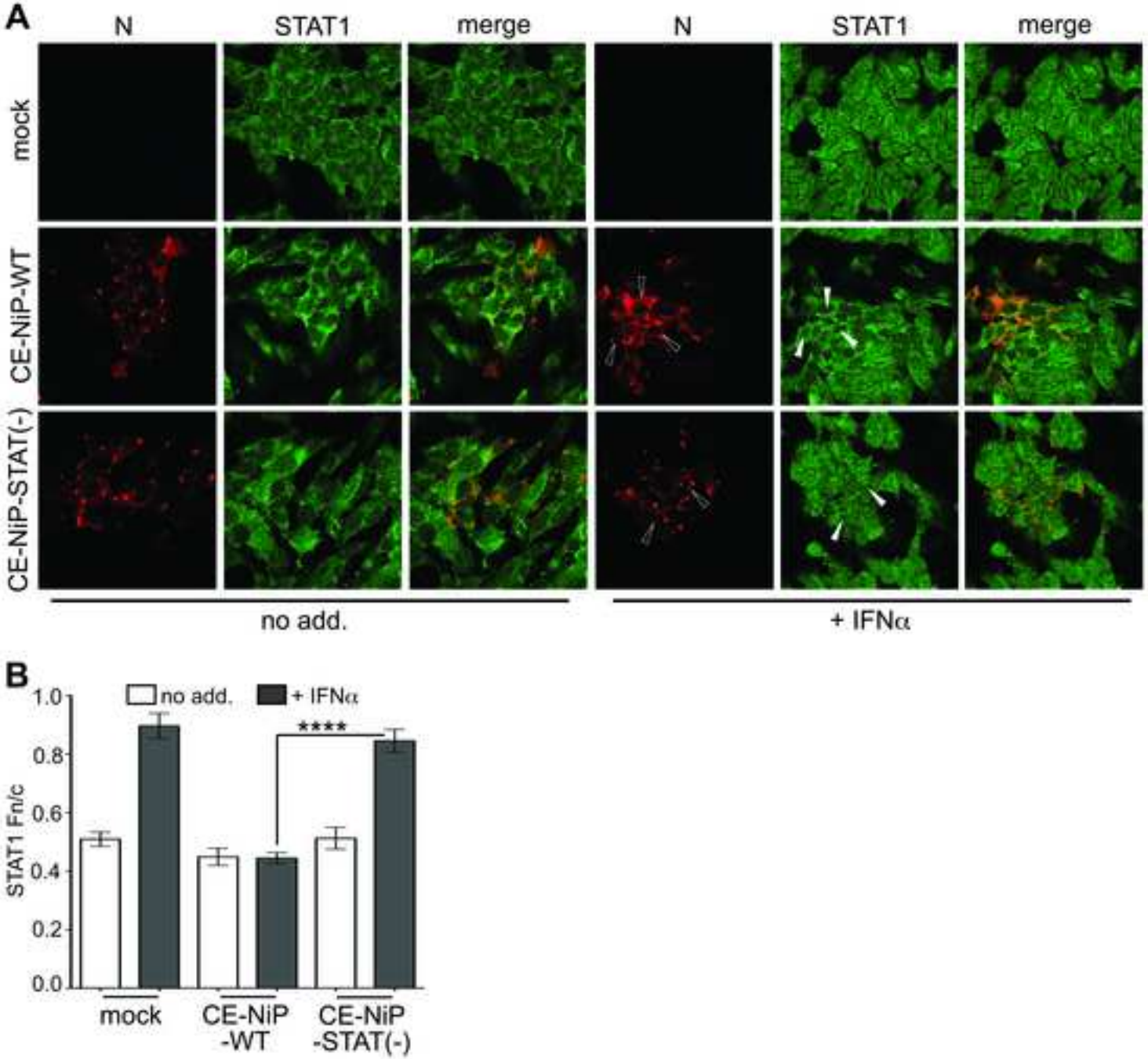

Figure 7
Click here to download high resolution image

Figure 7

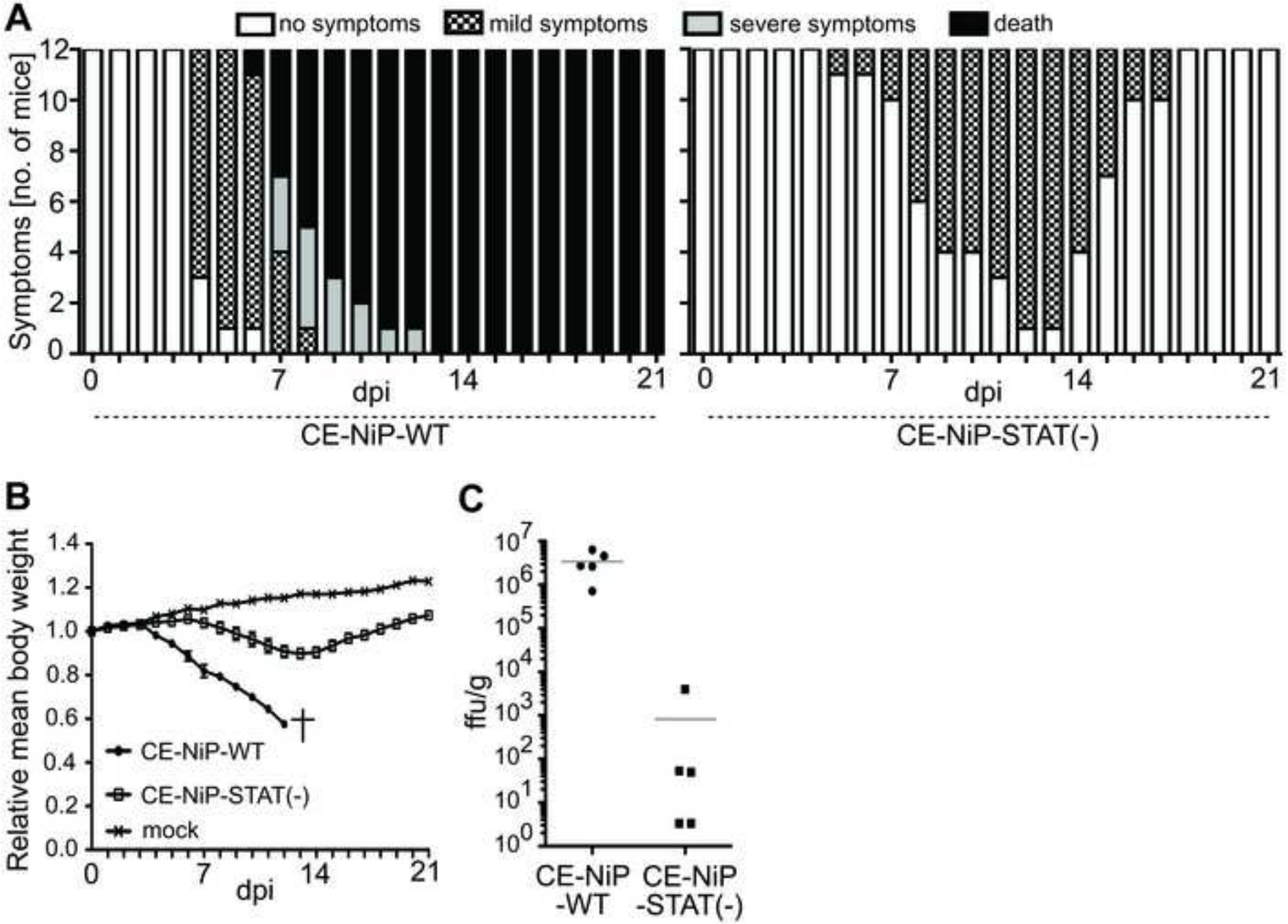

Supplementary Information

Supplementary Materials and Methods:

Constructs. Constructs to express RABV and DUVV full-length P-protein, RABV P-protein CTDs, RABV P-ΔC30, and RABV N-protein were generated by PCR from cDNA of the P-genes of RABV (CVS strain) and DUVV, or the N-gene of RABV (CVS strain) [1-4]. cDNA for RABV P-W265G, P-M287V, P-K214A/R260A, P-W265G/M287V, and DUVV P-M287V was generated by PCR overlap mutagenesis [5]. PCR products were cloned into the pEGFP-C1 or pmCherry-C1 (Clontech) for mammalian cell expression of protein fused to the C-terminus of GFP or mCherry. For yeast cell expression, PCR products were cloned into pLex plasmid (for P-protein CTD regions) and into pGAD plasmid (for N-protein), as previously described [6].

The pRVDI-luc minigenome construct contains a hCMV promoter upstream of cDNA fragments of a hammerhead ribozyme [7], the 5' trailer region of RABV (RC-HL strain), a firefly luciferase reporter gene, the 3' leader region of RABV (RC-HL strain), and a hepatitis delta virus (HDV) antigenomic ribozyme. Translation start and stop codons of the firefly luciferase gene are located in the same positions as those of N- and L-genes, respectively, in the RC-HL genome such that RNA transcripts acquire the authentic 3' and 5' terminal sequence of RC-HL genome after self-cleavage of hammerhead and HDV ribozymes. Helper plasmids were generated by cloning the complete cDNAs of RC-HL N-gene (pC-RN) or L-gene (pC-RL) into pCAGGS/MCS (kindly provided by Yoshihiro Kawaoka, University of Tokyo). Details of the plasmid construction are available from the authors on request.

Cell culture. Mammalian cells were cultured at 37°C, 5% CO^2 in DMEM with 10% FCS (Cos-7, HEK293T), EMEM with 10% FCS (NA, Vero, SK-N-SH), or EMEM supplemented with 10% tryptose phosphate broth and 5% FCS (BHK/T7-9).

Luciferase reporter gene assays. For IFN-dependent signaling assays, cells were cotransfected with 1µg pISRE-luc, 0.16µg pRL-TK and 1µg pEGFP-C1 encoding WT or mutant P-protein. Following treatment without or with IFNα (1000U/ml, 16 h), cells were lysed using passive lysis buffer (PLB, Promega) containing 1x PhosSTOP and 1x protease inhibitor (Roche Applied Science). Firefly and Renilla luciferase activity was determined and derived values for each sample were normalized to those for control samples (P-Δ30-transfected cells).

For minigenome assays cells were transfected with 0.8µg pRVDI-luc, 1.2µg pC-RN, 0.4µg pCRL and 0.12µg pEGFP-C1 encoding WT or mutant P-proteins and lysed in PLB before analysis of firefly activity.

qRT-PCR. To generate cDNA, total RNA isolated from transfected HEK293T cells (Qiagen RNeasy Mini Kit) was treated to remove DNA (DNA-free™ kit, Ambion) before reverse transcription using oligo$(dT)_{20}$ primer (SuperScript™ III First-Strand Synthesis system, Invitrogen). qRT-PCR analysis was performed using the SensiMix™ SYBR Hi-ROX kit (Bioline) with a 7900HT Fast Real-Time PCR system (Applied Biosystems). Standard curves were generated for each primer using serial dilutions of the reference cDNA (mock-transfected samples treated with IFNα). Data were normalized to *GAPDH* and the relative amount of mRNA was determined using the 2-ΔΔCT method [8]. PCR primers used to detect human *MxA*, *ISG15*, *GAPDH*, and *IFNβ* were used previously [9-12].

Immunoprecipitation. IP used the GFP-Trap® system, with lysis and wash buffer supplemented with 1x PhosSTOP and 1x protease inhibitor. IB analysis used antibodies for STAT1, STAT2, GFP, and mcherry (see below).

Y2H assays. For Y2H of P- and N-protein interaction, yeast cells (L40 strain) containing His3-and LacZ reporter genes were transformed with pLex plasmids to express P-protein CTDs fused to the DNA-binding domain of LexA (BD) and pGAD-N plasmid to express N-protein fused to the activation domain (AD) of *GAL4*. The P-N-protein interaction was assessed by the expression of the His3 reporter gene in yeast growing on media lacking tryptophan, leucine, and histidine, indicated by the appearance of blue colonies following growth for 1 to 18 h at 30°C in the presence of X-Gal mixture (0.5% agar, 0.1% SDS, 6% dimethylformamide and 0.04% X-Gal (5-bromo-4-chloro-3-indolyl-β-D-galactosidase)).

Growth curves and IFN sensitivity assays. Vero cells inoculated with virus (MOI of 0.001) were grown in 4ml culture media and 500µl supernatant was removed daily for titration by focus formation assay, and replaced with fresh media. In some assays fresh media contained 500U/ml IFNα after 1 day post inoculation.

Focus formation assays. Infected NA or Vero cells were fixed using 3.7% formaldehyde (10 min) and 90% methanol (5 min) before immunostaining with anti-RABV N-protein antibody (see below).

Mouse infection. Mice infected with 10^4 ffu of virus were monitored daily for symptoms of disease, which were classified as no symptoms, mild symptoms (>3% reduction of body weight, ataxia), severe symptoms (neurological manifestation, paralysis), and death. Body weight changes were calculated relative to the weight at 0

dpi. Mice failing to show righting reflexes in body tilt experiments (end-point) were sacrificed.

Immunostaining, confocal microscopy and image analysis. Cells grown on coverslips were infected with WT or mutant virus and treated without or with IFNα before fixation with 3.7% formaldehyde (10 min) and 90% methanol (5 min), and immunostaining (see below). Digitized confocal images (single sections sampled at the mid-point of the nucleus) were acquired using an Olympus FV1000 and analyzed using ImageJ 1.42 public domain software (NIH) to calculate the ratio of nuclear to cytoplasmic fluorescence corrected for background fluorescence (Fn/c) for individual cells, with mean Fn/c values calculated for >30 cells [2-4, 14-19].

Multiple sequence alignment analysis. Multiple sequence alignments were performed using ClustalW (UCD Dublin, Ireland).

Antibodies. Antibodies used for IB analysis were anti-STAT1 (BD Biosciences, catalog no. 610185), anti-STAT2 (Santa Cruz Biotechnology, catalog no. sc-22816), anti-GFP (Roche Applied Science, catalog no. 11814460001), and anti-mCherry (Abnova, catalog no. PAB18013), with HRP-conjugated Alexa-488- and 568-conjugated secondary antibodies.

Antibodies used for immunostaining were anti-STAT1 (Santa Cruz Biotechnology, sc-346), anti-RABV N-protein [13], anti-pY-STAT1 (Cell Signaling, cat. no. 9176), and anti-RABV P-protein (anti-P-protein rabbit serum, kindly provided by A. Kawai), with Alexa 488- and 568-conjugated secondary antibodies.

Structural analysis. The PDB file for the RABV P-protein CTD crystal structure (1VYI, [20]) was processed using the PyMol Molecular Graphics System software (1.5.0.4).

Supplementary References:

1. Delmas O, Holmes EC, Talbi C, et al. Genomic diversity and evolution of the lyssaviruses. PLoS One **2008**; 3:e2057.

2. Moseley GW, Filmer RP, DeJesus MA, Jans DA. Nucleocytoplasmic distribution of rabies virus P-protein is regulated by phosphorylation adjacent to C-terminal nuclear import and export signals. Biochemistry **2007**; 46:12053-61.

3. Moseley GW, Lahaye X, Roth DM, et al. Dual modes of rabies P-protein association with microtubules: a novel strategy to suppress the antiviral response. J Cell Sci **2009**; 122:3652-62.

4. Wiltzer L, Larrous F, Oksayan S, et al. Conservation of a Unique Mechanism of Immune Evasion across the Lyssavirus Genus. J Virol **2012**; 86:10194-9.

5. Ho SN, Hunt HD, Horton RM, Pullen JK, Pease LR. Site-directed mutagenesis by overlap extension using the polymerase chain reaction. Gene **1989**; 77:51-9.

6. Raux H, Flamand A, Blondel D. Interaction of the rabies virus P protein with the LC8 dynein light chain. J Virol **2000**; 74:10212-6.

7. Ruffner DE, Stormo GD, Uhlenbeck OC. Sequence requirements of the hammerhead RNA self-cleavage reaction. Biochemistry **1990**; 29:10695-702.

8. Schmittgen TD, Livak KJ. Analyzing real-time PCR data by the comparative C(T) method. Nat Protoc **2008**; 3:1101-8.

9. Kapadia SB, Brideau-Andersen A, Chisari FV. Interference of hepatitis C virus RNA replication by short interfering RNAs. Proc Natl Acad Sci U S A **2003**; 100:2014-8.

10. Shaw ML, Cardenas WB, Zamarin D, Palese P, Basler CF. Nuclear localization of the Nipah virus W protein allows for inhibition of both virus- and toll-like receptor 3-triggered signaling pathways. J Virol **2005**; 79:6078-88.

11. Vandesompele J, De Preter K, Pattyn F, et al. Accurate normalization of real-time quantitative RT-PCR data by geometric averaging of multiple internal control genes. Genome Biol **2002**; 3:RESEARCH0034.

12. Vandevenne P, Lebrun M, El Mjiyad N, et al. The varicella-zoster virus ORF47 kinase interferes with host innate immune response by inhibiting the activation of IRF3. PLoS One **2011**; 6:e16870.

13. Minamoto N, Tanaka H, Hishida M, et al. Linear and conformation-dependent antigenic sites on the nucleoprotein of rabies virus. Microbiol Immunol **1994**; 38:449-55.

14. Ito N, Moseley GW, Blondel D, et al. Role of interferon antagonist activity of rabies virus phosphoprotein in viral pathogenicity. J Virol **2010**; 84:6699-710.

15. Lieu KG, Brice A, Wiltzer L, et al. The Rabies Virus Interferon Antagonist P Protein Interacts with Activated STAT3 and Inhibits Gp130 Receptor Signaling. J Virol **2013**; 87:8261-5.

16. Moseley GW, Leyton DL, Glover DJ, Filmer RP, Jans DA. Enhancement of protein transduction-mediated nuclear delivery by interaction with dynein/microtubules. J Biotechnol **2010**; 145:222-5.

17. Moseley GW, Roth DM, DeJesus MA, et al. Dynein light chain association sequences can facilitate nuclear protein import. Mol Biol Cell **2007**; 18:3204-13.

18. Oksayan S, Wiltzer L, Rowe CL, Blondel D, Jans DA, Moseley GW. A novel nuclear trafficking module regulates the nucleocytoplasmic localization of the rabies virus interferon antagonist, P protein. J Biol Chem **2012**; 287:28112-21.

19. Roth DM, Moseley GW, Glover D, Pouton CW, Jans DA. A microtubule-facilitated nuclear import pathway for cancer regulatory proteins. Traffic **2007**; 8:673-86.

20. Mavrakis M, McCarthy AA, Roche S, Blondel D, Ruigrok RW. Structure and function of the C-terminal domain of the polymerase cofactor of rabies virus. J Mol Biol **2004**; 343:819-31.

Supplementary Figure Legends:

Figure S1. Analysis of the effect of mutations W265G/M287V and K214A/R260A on P-protein inhibition of STAT1 phosphorylation and interaction with STAT1/2. Cos-7 cells transfected to express the indicated GFP-fused P-proteins were treated without or with 1000U/ml IFNα (16h) before (A) lysis and IB for pY-STAT1 and GFP-fused P-protein, or (B) IP for GFP-fused P-protein and IB analysis of lysates (input) and IP for STAT1, STAT2 and GFP-fused P-proteins.

Movie S1. CE-NiP-STAT(-) virus does not cause symptoms of rabies. Mice that were i.c. mock-infected (yellow color) or infected with 10^4 ffu CE-NiP-WT virus (red color) or CE-NiP-STAT(-) (blue color) are shown at 7 dpi. Neurological symptoms are apparent for CE-NiP-WT-infected mice but not for mock- or CE-NiP-STAT(-)-infected mice.

Figure S1
Click here to download high resolution image

Supplementary Figure S1

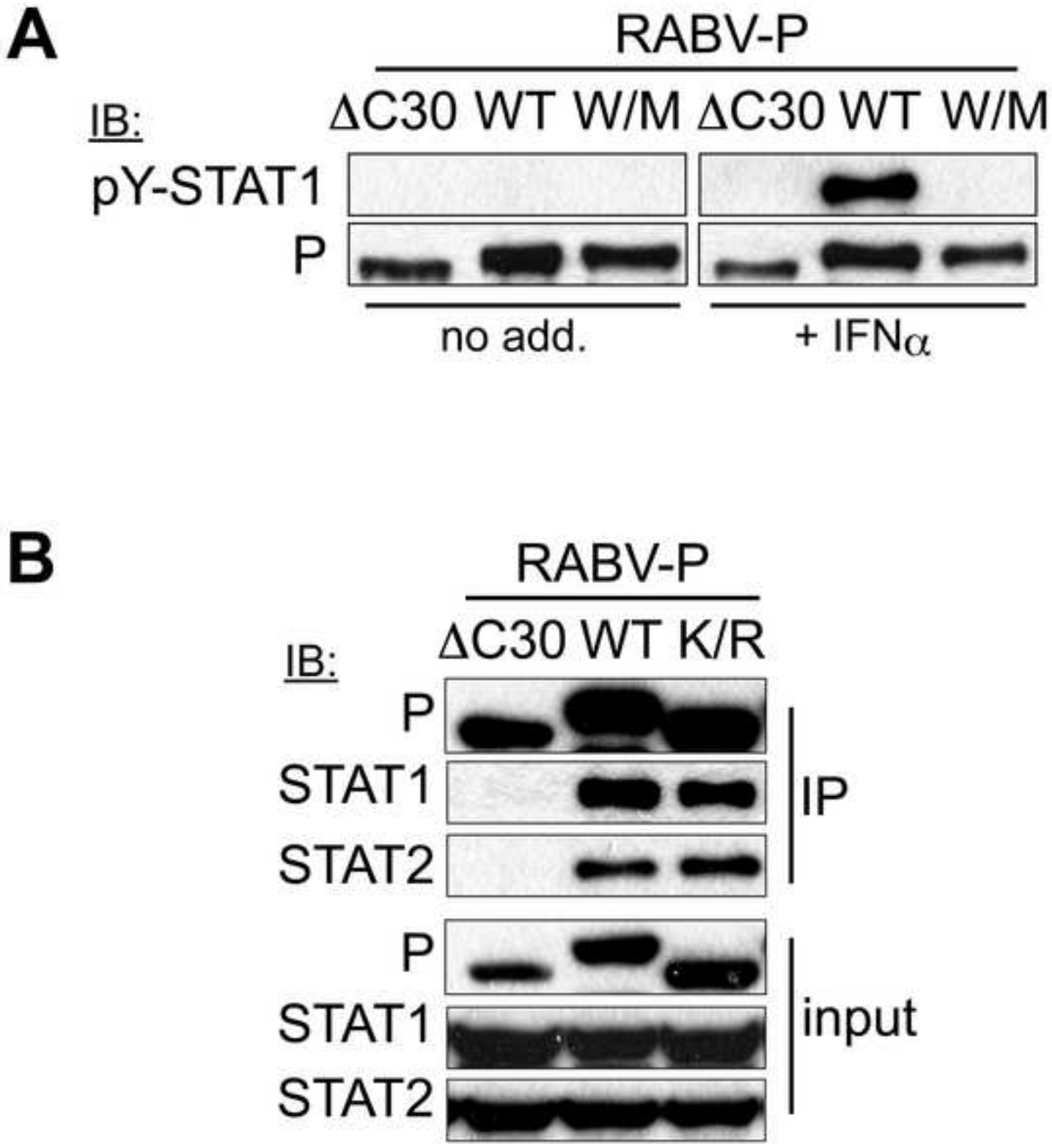

Video S1

Click here to download Video: Movie_S1.mov

Author/s:
Wiltzer, L; Okada, K; Yamaoka, S; Larrous, F; Kuusisto, HV; Sugiyama, M; Blondel, D; Bourhy, H; Jans, DA; Ito, N; Moseley, GW

Title:
Interaction of Rabies Virus P-Protein With STAT Proteins is Critical to Lethal Rabies Disease

Date:
2014-06-01

Citation:
Wiltzer, L., Okada, K., Yamaoka, S., Larrous, F., Kuusisto, H. V., Sugiyama, M., Blondel, D., Bourhy, H., Jans, D. A., Ito, N. & Moseley, G. W. (2014). Interaction of Rabies Virus P-Protein With STAT Proteins is Critical to Lethal Rabies Disease. JOURNAL OF INFECTIOUS DISEASES, 209 (11), pp.1744-1753. https://doi.org/10.1093/infdis/jit829.